This is an extended version of the paper presented in SEE8 conference, peer-reviewed again and approved by the JSEE editorial board.

Reliability Analysis of Seismic Stability of Gotvand Dam, Southwest of Iran

Mehdi Mohammadrajabi[1], Ghassem Habibagahi[2], Ali Shafiee[3], Seyed Mohammad Sadegh Sahraeian[4*], and Somayeh R. Tafti[5]

1. Design Engineer, Hayward Baker Inc., Nashville, USA
2. Professor, Department of Civil and Environmental Engineering, Shiraz University, Shiraz, Iran
3. Assistant Professor, Department of Civil Engineering, California State Polytechnic University, Pomona, USA
4. Assistant Professor, Department of Civil and Environmental Engineering, Shiraz University of Technology, Shiraz, Iran, * Corresponding Author; email: sahraeian@sutech.ac.ir
5. Research Assistant, Zachry Department of Civil Engineering, Texas A&M University, College Station, USA

Received: 26/06/2019
Accepted: 09/02/2020

ABSTRACT

Seismic design of an embankment dam is a vital step in the design procedure of this important infrastructure. Deterministic approaches such as quasi-static and Newmark method have been employed to evaluate slope stability of embankment dams. However, the variables required for a slope stability analysis, e.g. soil strength, pore pressure and loading parameters involve uncertainties which cannot be handled in the traditional deterministic methods. As an alternative, reliability analysis might be conducted to assess reliability indexes and the related failure probability of embankment dams. In this study, based on probability theories, a reliability analysis is performed to evaluate the seismic stability of an embankment dam (i.e., Gotvand dam) constructed in Iran. The probability of failure under seismic loading is considered for different sources of uncertainties involved in the problem, including uncertainty of loading, and the friction angle of core material as a strength parameter. Employing some statistical parameters, dynamic analysis is performed to determine the influence of friction angle variation on seismic slope stability. Significant pore pressure may build-up during cyclic loading, especially, when mixed clay (mixed clay and gravel) constitutes the dam core. Also, an undrained behavior of core materials has a great importance. Therefore, to estimate the effect of pore pressure build-up during seismic loading, two types of core materials (pure clay and mixed clay) are considered in this research. The results of dynamic analysis by finite element method are used to obtain the critical surface and acceleration in the embankment. Then, Newmark approach is employed to calculate the permanent displacement of the dam. Finally, reliability analysis is conducted and seismic performance of Gotvand dam during the earthquakes is investigated.

Keywords:
Reliability analysis; Newmark method; Seismic stability; Embankment dam; Deterministic approach; Uncertainty; Probability of failure; Reliability index

1. Introduction

Reliability analysis firstly introduced to the geotechnical field during the 1970s has widespread applications nowadays, while geotechnical issues include various types of uncertainties, e.g. material parameters and applied loads uncertainties. Some of the geotechnical fields in which this analysis has been employed are slope stability, foundations, soil liquefaction, landslides, etc. In other words, there is a growing need for rational approaches to treat uncertainties in geotechnics and take them into account for making an appropriate decision. Ayyub [1] discussed on different types of uncertainties in

geotechnics and explained how to encounter each type. Also, simple calculation tools for reliability and risk analyses in geotechnical engineering along with some examples are presented by Phoon and Ching [2]. Beer et al. [3] studied reliability analysis of geotechnical projects in case of scare information, using a comparison of alternative approaches. Moreover, Bea [4] proposed reliability based engineering approaches and strategies that might be employed to address different kinds of uncertainties in geotechnical engineering. Ranganathan [5] introduced various types of probabilistic procedures (First Order Second Moment (FOSM) and Monte Carlo Simulation Method (MCSM)) applicable in reliability analysis. Wolff [6] and Tang et al. [7] utilized probabilistic methods for slope stability analysis and employed FOSM for reliability analysis. Tobutt [8] studied slope stability and failure probability of an embankment using MCSM. Besides, a practical reliability analysis of slope stability using advanced Monte Carlo simulations is reported by Wang et al. [9]. Besides, Chowdhury and Xu [10] used probabilistic reliability analysis to obtain an optimum sliding face of slopes. These approaches are also employed for the design of embankment dams [11]. Furthermore, a reliability analysis of three-dimensional dynamic slope stability is reported by Al-Homouda and Tahtamonib [12]. In addition, some investigations about the reliability of slopes using Fuzzy sets are presented by Juang et al. [13] and Habibagahi and Shahgholian [14]. Seismic slope stability analysis, the topic of this research, includes lots of variables such as soil properties (e.g. shear strength parameters), geometry of the problem, location of water table, and seismic loading. Therefore, the design engineer has to deal with ambiguity and uncertainty that exist in these variables.

Currently, it is common to employ compacted gravel-clay mixtures as the core of embankment dams. Review of literature on the monotonic behavior of a mixture of clay and gravel indicates that generally shear strength (drained angle of friction) enhances with gravel content [15-17]. The previous investigation by Jafari and Shafiee [18] on gravel-clay and sand-clay mixtures confirmed prior outcomes on monotonic loadings. They showed that a considerable increase in coarse aggregate content significantly raised the excess pore water pressure in cyclic loading, which caused a reduction in cyclic shear strength.

Build-up of pore pressure in mixed clay (mixed clay and gravel) needs to be investigated carefully, especially for the seismic stability of embankment dams in which this hybrid material is used in the core. Seco e Pinto [19] showed that the main reason for damage or failure is the build-up of pore pressures with the consequent loss of shear strength in the embankment. Shafiee [20] and Shafiee et al. [21] showed how a noticeable increase in seismic pore pressure can reduce the factor of safety of dams with a mixed clay core. There are two main approaches in the literature for seismic slope stability analysis, namely dynamic analysis [22] and stress-deformation analysis [23]. Often, finite-element or finite-difference mathematical model is incorporated in these methods. In dynamic analyses, incorporating the proper model for soil behavior, the variation of acceleration in embankment height, pore pressure build-up, and cyclic degradation of shear strength, the variation of factor of safety against time is calculated during an earthquake.

In this study, a new approach is implemented to evaluate the displacement-based seismic stability of Gotvand dam, southwest of Iran using a reliability analysis. In order to investigate the effect of remarkable pore pressure build-up triggered by seismic loading in the mixed clay core on the stability of the dam, two types of core materials, pure clay and mixed clay were modeled. The uncertainties were attributed to the friction angle of core materials and seismic loading as the representatives of capacity and demand, respectively. The Newmark sliding block approach, first introduced in 1965 [24], was utilized to estimate the permanent displacement of the dam under excitation of 10 earthquake records.

2. General Specifications of Gotvand Dam

Gotvand dam located in the south west of Iran in Khuzestan Province is a 180 m height embankment dam with central clayey core and a crest length of 760 m. The dam construction site is mostly composed of rock materials of Aghajari formation. The site includes successive layers of fine grain material with medium to coarse grain Sandstone and Conglomerate. The fine grain

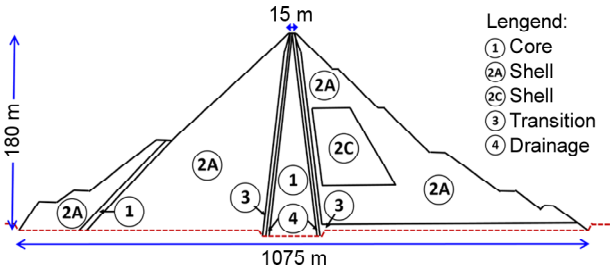

Figure 1. Typical cross-section of Gotvand dam [25].

material is formed by Marl, Siltstone and thin layers of Sandstone. The total volume of the reservoir is 4500 MCM and the reservoir area is about 96.5 km^2. The project has a hydropower station with 250 MW units, and three diversion tunnels in the left bank. A schematic cross-section of the dam is shown in Figure (1). According to ICOLD (International Commission on Large Dams) guidelines, the dam is classified as a large dam. Following the successful application of gravel-clay mixtures as the cores of many embankment dams in Iran, it was decided to use such materials as the core of Gotvand dam. On the basis of laboratory tests [25], it was decided to use a combination of 60% clay and 40% sandy gravel as the core material. Further studies on the mixed clay and gravel [18, 20-21] revealed a high potential for pore pressure build-up in cyclic loading when the aggregate content is equal to or greater than 40%. This fact indicates the importance of dynamic analysis to evaluate the effect of pore pressure build-up on the seismic stability of Gotvand dam.

3. Modeling of Mixed Clays and Gravel

In this study, two types of core materials, i.e., clay-gravel mixture and pure clay were used to investigate the effect of pore pressure build-up during seismic loading on the stability of the dam. The results of triaxial tests conducted by Jafari and Shafiee [18] were used to obtain the appropriate soil parameters for the analyses. They adopted a specimen preparation procedure to resemble the in-situ conditions of the core material of the embankment dam. The specimens, 50 mm in diameter and 100 mm in height, were compacted in six layers with a dry density of 95% of maximum dry density obtained from the standard compaction test method (ASTM1999) and water content 2% wet of optimum value. Two samples of Clay-Gravel mixture were mixed in volumetric proportion. The specimens were saturated with a Skempton B-value in excess of 95%, and then were isotropically consolidated under three different effective confining stress of 100, 300 and 500 kPa. Following consolidation, undrained monotonic triaxial tests were carried out under strain-controlled condition. Then, a back analysis was carried out to find the appropriate soil parameters, so that the same specimen was modeled in the PLAXIS software, and the soil parameters were varied until the satisfactory consistency was achieved between test results and the numerical analysis.

The hardening soil model was used to simulate undrained triaxial tests. This model is very useful, especially when it is applied to the analyses of embankments, considering the difficulties associated with the laboratory testing of materials. The calculations were performed for two different sets of materials, pure clay and mixed clay, with different material parameters till the best-fitted parameters were obtained through comparing the results of the tests with PLAXIS results (Figure 2). The results of experimental research program were used to calibrate the PLAXIS model. The calibrated parameters for core materials (pure clay and mixed clay) are presented in Table (1). Moreover, the parameters of the material model for crest, filter and transition are presented in this table. Using these materials, Gotvand dam was modeled in PLAXIS2D V.9.0, and dynamic analyses were conducted on the model.

4. Seismic Hazard Analysis and Earthquake Records Selection

A summary of seismic hazard analysis for this site conducted by Mahab-Ghods consulting engineering company [26] is presented in Table (2). Based on the seismic hazard report, PGAs for the project location are 0.27 g and 0.48 g for the design basis earthquake (DBL) and maximum credible earthquake (MCL), respectively (Table 2). Also, due to the existence of the active Lahbari fault at a distance of less than 10 km to the dam site, this project lies in the class IV of hazard category [26]. Therefore, according to the ICOLD recommendations, time histories-based analyses are mandatory to specify and represent fault specific phenomena

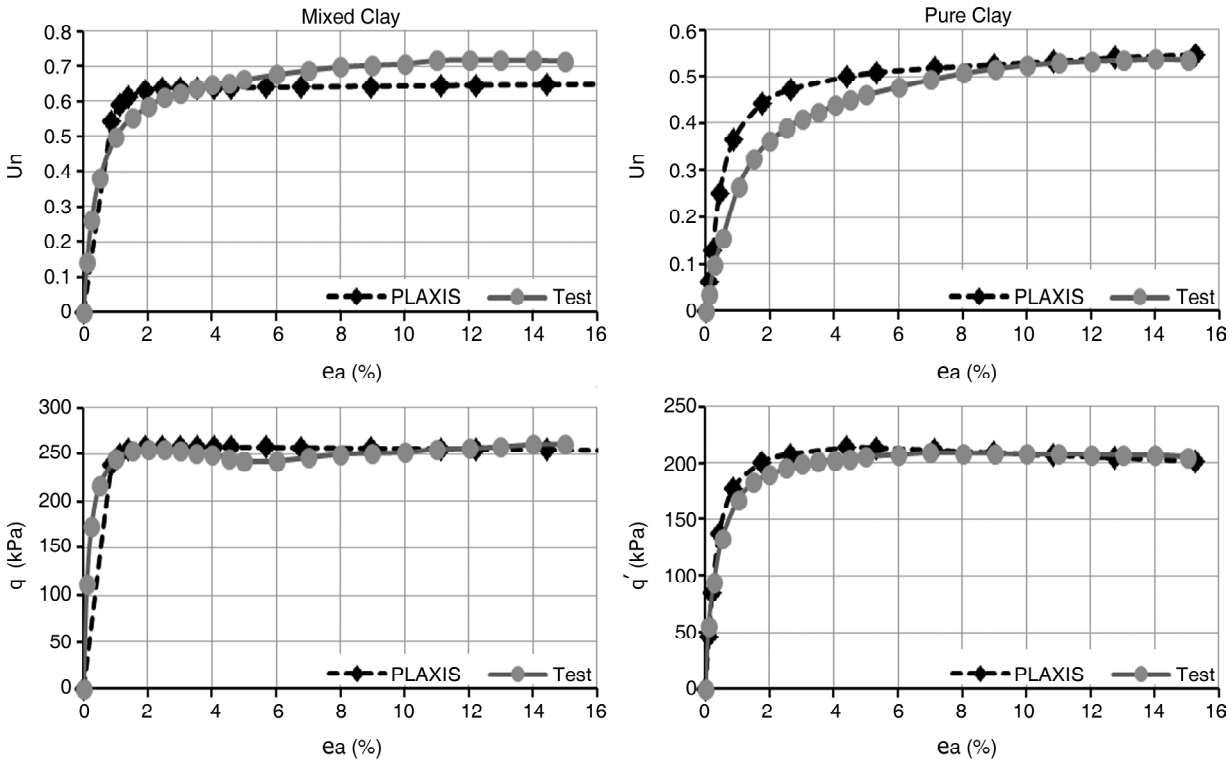

Figure 2. Comparison between the test and PLAXIS results on the calibration and determination of the material properties (a) mixed clay (b) pure clay (in P0=300kPa).

Table 1. Material properties of core and body of embankment.

	Core Materials		Body Materials		
Parameter	**Pure Clay**	**Mixed Clay**	**Zone (2A)**	**Zone (2C)**	**Filter**
Cohesion C(kPa)	0	0	0.2	0.2	0.2
Friction angle φ(degree)	24.7	32.5	44	35	30
Dilation angle (ψ)	0	0	14	5	0
Module of Elasticity E_{50}^{ref}(kPa)	7000	31000	1.08e5	6.54e4	4.63e4
Module of Elasticity E_{oed}^{ref}(kPa)	4239	23960	1.08e5	6.57e4	4.63e4
Module of Elasticity E_{ur}^{ref}(kPa)	1.93e4	9.9e4	3.24e5	1.971e5	1.389e5
υ_{ur}	0.2	0.25	0.3	0.2	0.25
P^{ref}(kPa)	100	100	100	100	100
K_0^{nc}	0.636	0.436	0.318	0.426	0.424
R_f	0.9	0.9	0.9	0.9	0.9
Saturated Unit Weight γ_{sat}(kN/m^3)	16	19	25	24	24
Unit Weight γ(kN/m^3)	13.5	16.9	21.5	20	20
X-Direction Conductivity K_X(m/day)	8.64e-5	8.64e-5	8.64	0.8	8.64e-4
Y-Direction Conductivity K_Y(m/day)	4.32e-5	4.32e-5	4.32	0.4	4.32e-4

and to account for potentially critical foundation conditions. Based on the faulting specification in the location of dam, in order to conduct dynamic analysis, ten earthquake records were selected as input motions in the analyses (Table 3). Then, the ten records were scaled to give the desired PGA of 0.27 g and 0.48 g appropriate to the project site, and they were employed as the shaking input to the base of the finite element model.

5. Newmark Sliding Block Method

5.1. Methodology

The most common approach to evaluate seismic deformation is the rigid block analysis described by Newmark [24]. He proposed a practical means for predicting slope movements during earthquakes,

Table 2. Peak ground acceleration [26].

Design Level	Return Period	PGA (g)
DBL	500	0.27
MCL	-	0.48

based on the analogy of a sliding block. Newmark's approach has been used extensively by numerous authors such as Makdisi and Seed [27], Jibson [28] and Wilson and Keefer [29]. The method was originally developed to measure permanent displacement in earthquakes but has been applied to assess a variety of slopes issues including lateral spreading.

In this article, a computer program was developed to estimate the Newmark displacement. A mean acceleration obtained from the dynamic analysis (PLAXIS) and yield acceleration obtained from GEO-STUDIO 2012 (GeoSlope) analysis were used as the inputs of the program. To calculate the mean acceleration, first, the slip surface was divided into ten slices and then, the center of each slice was determined. Next, the result of dynamic analysis was obtained in these selected central points, finally, a weighted average was applied to calculate the mean acceleration for the critical slip surface. Using the mean acceleration, the permanent displacement of the blocks was obtained by integrating the acceleration time history above the yield acceleration. A typical graph for the methodology applied in this study is presented in Figure (3).

The effect of pore pressure build-up on the permanent deformation during the earthquakes was also studied in the dynamic analysis. To check the influence of mixed clay as the core of the dam, these calculations was made not only for pure clay core,

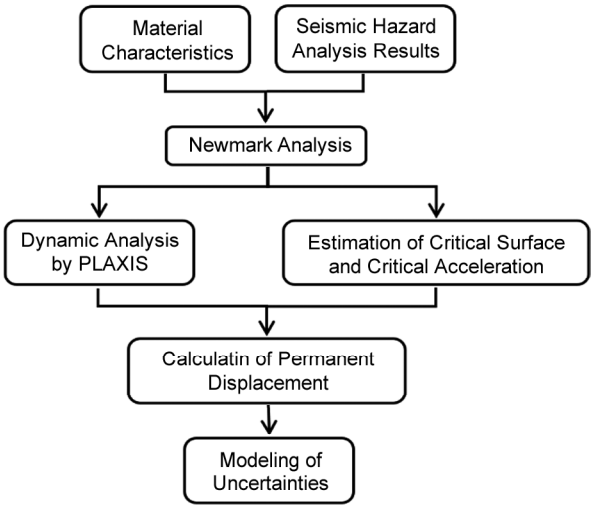

Figure 3. Methodology of the study.

but also for mixed clay-gravel core and the results were compared. A sensitivity analysis is required to find out the influence of variation of friction angle on the permanent displacement. Therefore, the dynamic analysis was conducted with different values of friction angle estimated by statistical analysis.

5.1.1. Estimation of Critical Sliding Surface

Although pseudo static method is proposed for estimation of critical slip surface, in this study, another approach is employed to obtain this surface. Because pseudo-static method cannot consider the change in material parameters during earthquakes, the critical surface in this study is obtained by an additional dynamic analysis using GEO-STUDIO software (Geo-Slope). To this end, the analysis was conducted for the ten selected accelerograms and yield acceleration along with critical slip surface was obtained. In the other words, the results of this analysis were utilized to obtain the points on the

Table 3. Accelerograms used in dynamic analysis.

Earthquake	Recording Station	Magnitude	Event Date	Epicentral Distance (km)
Irpinia, Italy	Sturno	6.5	1980/11/23	32.0
Kocaeli, Turkey	Izmit	7.8	1999/08/17	4.8
Cape Mendocino	89486 Fortuna	7.1	1992/04/25	13.7
Chi-Chi, Taiwan	PNG	7.6	1999/09/20	114.21
Spitak, Armenia	12 Gukasian	7.0	1988/12/07	30.0
Chi-Chi, Taiwan	ALS	7.6	1999/09/20	15.29
Kobe	0 Kakogawa	6.9	1995/01/16	26.4
Loma Prieta	47125 Capitola	6.9	1989/10/18	14.5
Georgia, USSR	18 Ambralauri	6.2	1991/06/15	73.7
Landers	90019 San Gabriel	7.4	1992/06/28	141.6

critical slip surface. These points are used to estimate the mean acceleration of the sliding wedge by finite element modeling as the input of Newmark approach discussed later. These analyses were carried out for the two types of materials; mixed clay and pure clay. The results showed that the difference between critical sliding surface and yield acceleration for two materials was not significant. A typical critical sliding surface is presented in Figure (4) and the results of yield accelerations are shown in Table (4).

5.1.2. Finite Element Model

Having the critical sliding surface, finite element model was generated using PLAXIS based on the cross section of Gotvand dam. A two-dimensional model is employed for plane strain analysis of the dam model because the ratio of dam's length and height is 4.2 and dam is located on the ground with high elastic modulus (rock material). This analysis was carried out for 10 accelerations with two seismic hazard levels (DBL and MCL) and two types of material with five values of friction angle.

Table 4. Newmark analysis results.

Earthquake	Yield Acceleration (g)	φ (degree)	Permanent Displacement (cm)			
			Pure Clay		Mixed Clay	
			DBL	MDL	DBL	MDL
Irpinia, Italy (1980)	1.28	21.33	0.4	26	9	92
		22.85	0.35	26	8	90
		24.7	0.31	27	8.5	90
		26.55	0.3	29	9	91
		28.07	0.27	29	9	92
Kocaeli, Turkey (1999)	1.3	21.33	1.2	37	12	71
		22.85	0.9	33	13	69
		24.7	1	33	12.3	71
		26.55	0.6	34	13	69
		28.07	0.8	29	14	70
Cape Mendocino (1992)	1.27	21.33	7.5	87	20	126
		22.85	8.7	88	21	125
		24.7	8	83	25	127
		26.55	8.5	84	25	135
		28.07	5	81	23	134
Chi-Chi, Taiwan (1999) (PNG)	1.3	21.33	0.02	28	6	90
		22.85	0.3	22	7	82
		24.7	0.1	28	6	78
		26.55	0.2	31	7	76
		28.07	0	25	7	78
Spitak, Armenia (1988)	1.27	21.33	0.5	16	0.04	19
		22.85	0.5	16	0.2	19
		24.7	0.6	17	0.2	20
		26.55	0.3	17	0.03	15
		28.07	0.3	16	0.2	15
Chi-Chi, Taiwan (1999) (ALS)	1.3	21.33	38	151	29	189
		22.85	34	150	31	190
		24.7	30	148	28	190
		26.55	30	137	28	187
		28.07	34	142	28	184
Kobe (1995)	1.27	21.33	0.2	6	0.9	14
		22.85	0.2	5	1	15
		24.7	0.2	5	1	14
		26.55	0.2	5	1.1	13
		28.07	0.2	5	1.3	14
Loma Prieta (1989)	1.27	21.33	0.8	17	0.13	19
		22.85	0.7	20	0.17	19
		24.7	0.7	19	0.16	17
		26.55	0.5	18	0.14	16
		28.07	0.4	17	0.17	17
Georgia, USSR (1991)	1.3	21.33	0.1	30	1	37
		22.85	0.2	29	1	36
		24.7	0.2	23	1	36
		26.55	0.1	22	2	37
		28.07	0.2	20	1	35
Landers (1992)	1.36	21.33	85	410	125	480
		22.85	72	406	122	463
		24.7	78	412	122	462
		26.55	73	410	131	486
		28.07	72	401	127	480

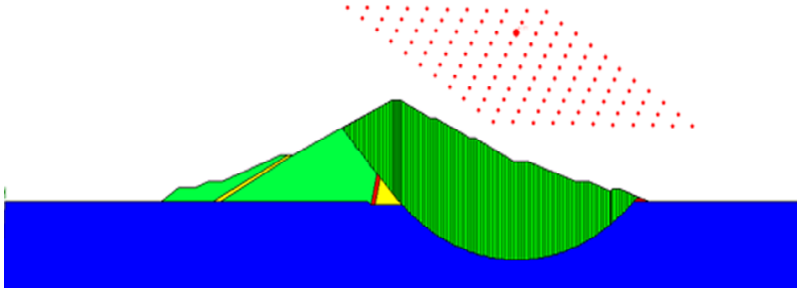

Figure 4. Critical slip surface.

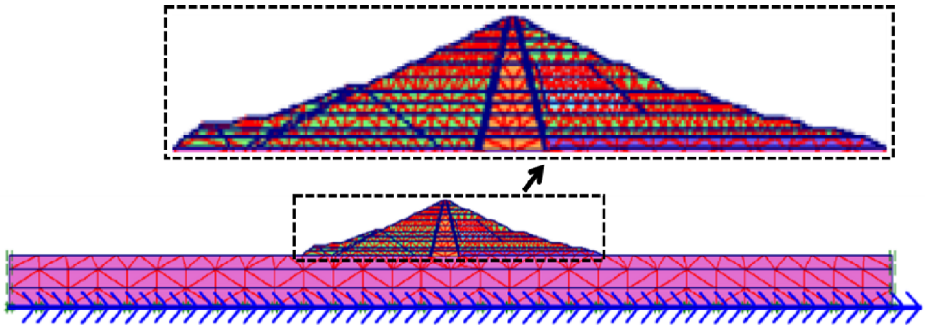

Figure 5. Finite element mesh of the embankment dam (PLAXIS 2D).

The finite element mesh with appropriate boundary condition was used in the analyses. To this end, the dam is divided into 11 layers with 1081 elements and 2318 nodes as shown in Figure (5). The elements were Trilateral with six nodes. The effect of number of elements and nodes on stresses and strains in the structure is investigated during the analysis to consider the sufficiency of the number of elements and nodes. While five different mesh sizes (extra-large, large, medium, fine and extra-fine) can be applied in the software (PLAXIS), the modeling is conducted using all these sizes, and the optimum mesh size that less affects the results is chosen. The foundation material was modeled as linear elastic material. The foundation was extended laterally enough (1 km each side), to ensure no wave is reflected from lateral boundaries. The thickness of foundation was considered 100 m. The foundation thickness was extended enough to ensure, the seismic bedrock (shear-wave velocity>760 m/s) is achieved. The main reason behind utilizing PLAXIS for dynamic analysis was employing appropriate constitutive models (Hardening model) to obtain more reliable results. Water pressure was applied at full operation head on the upstream face and at ground level on the downstream side of the embankment.

The core material was assumed to be saturated mixed clay-gravel and pure clay with the undrained shear strength characteristic provided by the laboratory study (Table 1). Analyses consisted of consolidation followed by seepage, and finally dynamic analyses. For Newmark analyses, acceleration time history of at least ten points within the sliding surface was needed. Thus, the average of ten points obtained by PLAXIS analysis is then applied in the Newmark sliding calculation.

5.2. The Results of Newmark Analyses

Figure (6) shows a sample of Newmark analysis results for two types of core materials, at DBL when Georgia time history record is applied at the base of the dam. The permanent displacements calculated for 200 cases and other detailed results are presented in Table (4). From these results, the influence of friction angle and excess pore pressure build-up on seismic deformation of Gotvand dam is discussed in detail in the next sections.

5.2.1. The Influence of Friction Angle

The effect of friction angle uncertainties on permanent displacement and seismic stability of embankment dam is investigated briefly in this research. For this purpose coefficient of variation (COV) of core materials for both materials in this research were estimated based on the results of

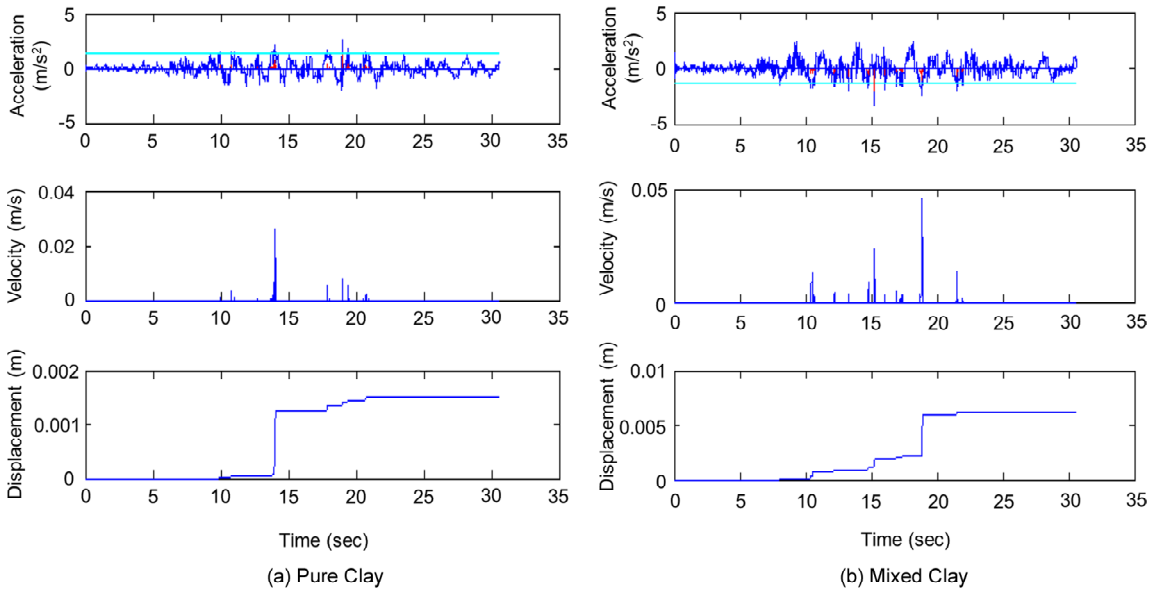

Figure 6. Newmark analysis result for Georgia (ay=1.3 g) (a) Pure clay core, (b) Mixed clay core in DBL.

Table 5. Variations of friction angle used in dynamic analysis.

Material	COV (%)	φ_1	φ_2	φ_3	φ_4	φ_5
Pure Clay	21	21.33	22.85	24.7	26.55	28.07
Mixed Clay	9	29.5	31	32.5	34	35.5

previous studies [30]. Then, using Equation (1), five values were calculated for each type of core material, shown in Table (5).

$$X_{new} = \bar{x} \pm \alpha \times \frac{\bar{x} \times COV}{\sqrt{n}} \quad (1)$$

where X_{new} is a new value of friction angle, $\bar{x}$ is mean value of friction angles, α is error, COV is coefficient of variation, and n is number of the data.

Since all the analyses were carried out under effective stress condition, and also the clay core was assumed to be normally consolidated, friction angle is considered as the most important shear strength parameter whose variation might affect the stability. The maximum deviation of permanent displacement, for different friction angles, from the value corresponding to the average friction angle is presented in Table (6). The influence of friction angle variation on permanent displacement of the embankment under a typical earthquake excitation is presented in Figure (7). A comparison between the variations of permanent deformation determined by Newmark analyses for two types of materials (i.e., mixed clay and pure clay) and for two levels of seismic hazard is presented in Figure (8). It is interesting to note,

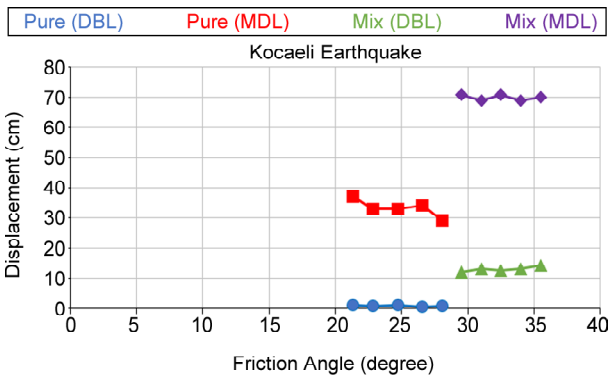

Figure 7. Variation of permanent displacement by different friction angle.

although the friction angle in the dam with mixed clay core is more than that with pure clay core, the permanent displacement in mixed clay core is more than that of the pure clay core (Figure 8). This is due to the fact that the excess pore pressure build-up in the mixed clay reduces the undrained shear strength substantially resulting in higher permanent displacement. Another point in this figure is the higher values of displacements for Landers earthquake, which is due to that in this accelerogram most part of the motion is above yield acceleration and caused greater values of permanent displacements.

Table 6. Influence of Friction angle on the permanent displacement.

Earthquake	Maximum Deviation from Permanent Displacement of Average Friction Angle	Pure Clay		Mixed Clay	
		DBL	MCL	DBL	MCL
Irpinia, Italy	ΔD(max) (cm)	0	2	0.5	2
	ΔD(max) (percent)	0	7.4	5.8	2.2
Kocaeli, Turkey	ΔD(max) (cm)	0	4	1.7	2
	ΔD(max) (percent)	0	12	13.8	2.8
Cape Mendocino	ΔD(max) (cm)	3	5	5	8
	ΔD(max) (percent)	6.2	6	20	6.2
Chi-Chi, Taiwan-PNG	ΔD(max) (cm)	0	6	1	12
	ΔD(max) (percent)	0	21	16.6	15.3
Spitak, Armenia	ΔD(max) (cm)	0	1	0	5
	ΔD(max) (percent)	0	5.8	0	25
Chi-Chi, Taiwan-ALS	ΔD(max) (cm)	8	11	3	6
	ΔD(max) (percent)	26	7	10	3
Kobe	ΔD(max) (cm)	0	1	0	1
	ΔD(max) (percent)	0	20	0	7.14
Loma Prieta	ΔD(max) (cm)	0	2	0	2
	ΔD(max) (percent)	0	10.5	0	11.2
Georgia, USSR	ΔD(max) (cm)	0	7	0	1
	ΔD(max) (percent)	0	30	0	2.7
Landers	ΔD(max) (cm)	7	11	9	24
	ΔD(max) (percent)	8.9	2.7	7.3	5.1

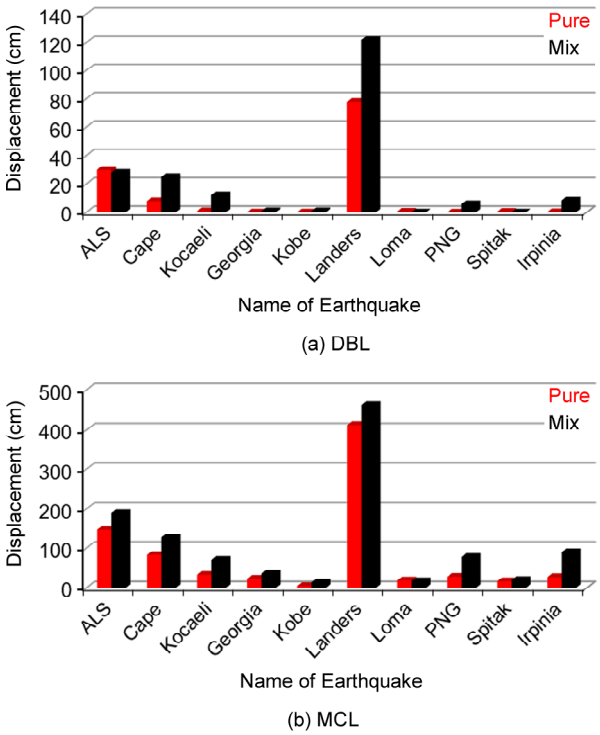

Figure 8. Clustered column of the permanent displacement for two types of material in (a) DBL, (b) MCL.

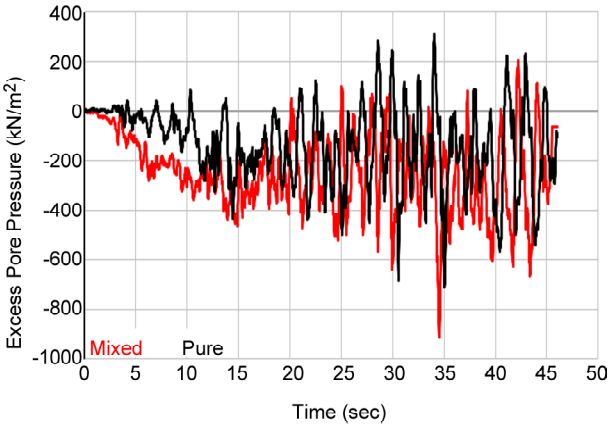

Figure 9. Excess pore pressure build-up during Landers earthquake versus time for mix and pure clay in MCL.

5.2.2. The Influence of Excess Pore Pressure

Variations of excess pore pressure build-up, within the mid-width of the dam core subjected to a typical earthquake record, are shown in Figure (9) (at elevation 115 m of core zone). The result of this dynamic analysis confirms the test results reported by Jafari and Shafiee [18]. The excess pore pressure build-up during an earthquake, in the mixed materials is more than that in the pure clay. The results of Newmark analyses show that the increase in pore pressure leads to an increase in permanent displacement (Table 4), and finally, this factor could threaten the seismic stability of dams. As a result, care should be taken in using mixed clays as the core of an embankment. Considering the inherent uncertainties in the capacity and demand parameters, the factor of safety may even fall below unity.

6. Modeling of Uncertainty

In geotechnical engineering, the reliability analysis of earth fills (e.g. embankments) can be performed using Bayesian updating technique in conjunction with a conditional random field to evaluate the uncertainty related to the spatial variation of the material properties within a dam based on quality control results during the construction [31-32]. Thus, the mathematical expectation and variance of the average shear strength along failure surface have been estimated from these results. Standard quality control programs have incorporated the results of control tests in reliability analysis as soon as they were available in order to make a decision based on the actualized evaluation of the reliability of earth structures [31, 33]. Stochastic finite element method (SFEM) is a good alternative for solving the geotechnical problem associated with material variability [34].

Recently, Random Finite Element Method (RFEM) has been introduced to solve a variety of practical problems in geotechnical engineering design. RFEM combines random field theory [35] with the finite element method [36] and Monte Carlo simulation to produce probabilistic results. Mrabet [37] and Mrabet and Bouayed [38] have used a methodology based on random field theory in conjunction with stochastic finite element method (SFEM) to describe the uncertainty in both the input material properties of a geotechnical system and the result of the analysis of an embankment dam.

The reliability analysis in geotechnical engineering is estimating the probability of failure (or reliability index) of a structure or a system. The reliability index of an embankment is commonly taken as the value corresponding to the failure surface associated with a minimum reliability index. Thus, the conventional factor of safety is defined as the ratio of the limit capacity of soil to a demand in terms of loads:

$$F = R/S \tag{2}$$

where R = capacity (resisting force or resisting moment); and S = demand (driving force or driving moment). In probabilistic modeling of safety, R and S are assumed to be random variables. Let $fR(r)$ and $fS(s)$ be the probability density functions of variables R and S. The probabilistic measure of safety is the probability of failure, P_f defined as (failure occurs if $R < S$):

$$P_f = P\left(\frac{R}{S} \le 1\right) \tag{3}$$

Then the reliability index, β, is defined as [39]:

$$\beta = \frac{E\{MS\}}{\sigma_{MS}} \tag{4}$$

in which $E\{MS\}$ = expected value of MS, and σ_{MS} = standard deviation of the normal distribution of MS. MS in this study is the difference between critical displacement ($D_{critical}$) and average normal distribution of displacement (μ_D). This provides a simple quantitative basis for assessing risk, i.e. probability of failure.

6.1. Methodology

The results obtained from dynamic and Newmark displacement analyses indicated that the effect of change in friction angle on the displacement is not so critical (Figure 7); therefore in this study, the related uncertainty is not investigated. Hence, only the uncertainty in the seismic loading is considered. To assess the uncertainty of loading in the seismic stability of embankment dam, a parameter of strong ground motion is required that could capture the whole effect of seismic loading on the stability of the dam. Herein, Arias intensity is selected as a ground motion parameter that captures the potential destructiveness of an earthquake as the integral of the square of the acceleration-time history related to the loading. Arias Intensity is defined by Arias [23] as:

$$I_a = \frac{\pi}{2g}\int_0^{\infty} a(t)^2 dt \tag{5}$$

where I_a is the Arias Intensity in units of length per time, $a(t)$ is the acceleration-time history in units of g, and g is the acceleration of gravity. The Arias intensities of 10 earthquake records are shown in Table (7).

On the other hand, a parameter is required to represent the structural properties, for instance, geometry, and strength of the material. The selected parameter is a predominant period (T_1) of structure (embankment). Another parameter applied in this

study as an independent variable is the predominant period of an earthquake (T_s) to identify the resonance frequency and use it in the probability distribution function (Table 7).

6.2. Probability Density Function

Three parameters, i.e., Arias Intensity, the predominant period of the dam, and the predominant period of earthquakes are considered as independent variables to derive the probability density function. The relationship between an independent parameter of $Arias \times T_S / T_1$ and dependent parameter, i.e., permanent displacement is illustrated in Figure (10). As shown, there is a good relationship between $Arias \times T_S / T_1$ and the permanent displacement, in such a manner that the permanent displacement increases when $Arias \times T_S / T_1$ increases. Four formulas are derived for two types of core materials,

Table 7. Earthquake parameters and predominant period of the dam.

Earthquake	Arias Intensity (m/s)		T_S (s)	T_1 (s)	
	DBL	MCL		Mixed Clay	Pure Clay
Irpinia, Italy	1.044	3.3	0.38	2.27	2.56
Kocaeli, Turkey	1.32	4.17	0.28	2.27	2.56
Cape Mendocino	1	3.19	0.46	2.27	2.56
Chi-Chi, Taiwan-PNG	3.11	9.83	0.12	2.27	2.56
Spitak, Armenia	0.579	1.82	0.34	2.27	2.56
Chi-Chi, Taiwan-ALS	1.714	5.44	0.54	2.27	2.56
Kobe	1.153	3.64	0.16	2.27	2.56
Loma Prieta	1.184	3.74	0.28	2.27	2.56
Georgia, USSR	1.62	5.13	0.42	2.27	2.56
Landers	3.04	9.49	0.82	2.27	2.56

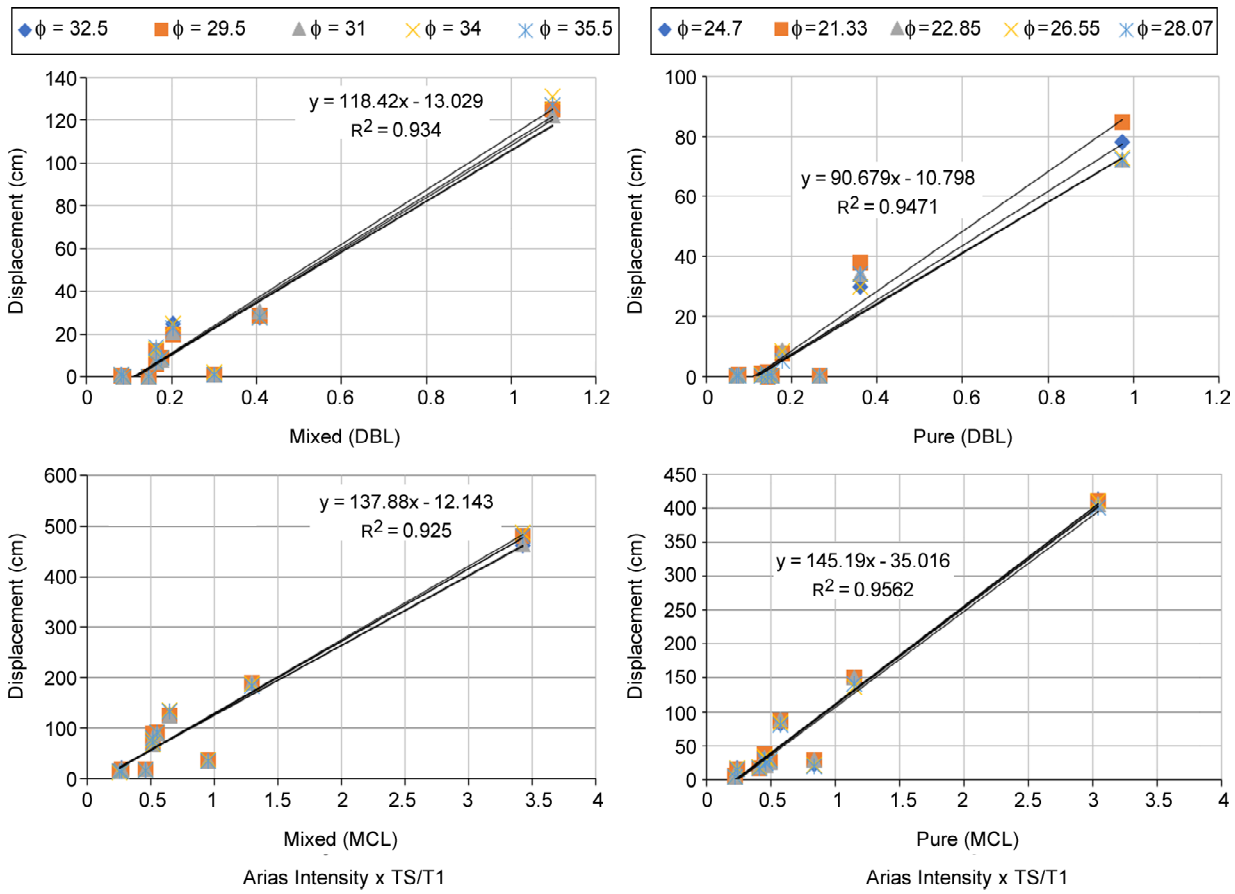

Figure 10. Permanent displacement versus Arias* T_S/T_1 for mix and pure clay in DBL and MCL.

Table 8. Formulas derived for permanent displacement.

Material	Level of Seismic Hazard	Function
Pure Clay	DBL	$D = 90.67 \times ARIAS \times \frac{T_S}{T_1} - 10.79$
	MCL	$D = 145.1 \times ARIAS \times \frac{T_S}{T_1} - 35.01$
Mixed Clay	DBL	$D = 118.4 \times ARIAS \times \frac{T_S}{T_1} - 13.02$
	MCL	$D = 137.8 \times ARIAS \times \frac{T_S}{T_1} - 12.14$

mixed clay and pure clay in two levels of seismic hazard, MCL and DBL (Table 8). The negligible effect of friction angle on the permanent displacement can also be verified as shown in Figure (10).

6.3. Probability Density Function for Independent Parameters (Input Data)

Herein, the probabilistic distribution of input parameters (Arias intensity and T_S/T_1) is determined. Because obtaining an appropriate distribution is required to expand the number of data, more accelerograms compatible with the seismotectonic and geology of the dam site are selected (Table 9). These accelerograms were normalized to DBL and MCL hazard levels. Using MINITAB software, distribution of Arias intensity and T_S/T_1 were obtained. The histogram of T_S/T_1 parameter for pure clay core is shown in Figure (11a) and the normal and lognormal distribution fitted to the histogram of T_S/T_1 are displayed in Figure (11b). In order to determine the compatible distribution for T_S/T_1, the Anderson-darling normality test was performed and the results of these tests illustrated in Figure (11c) indicate that the lognormal distribution is suitable for independent variable T_S/T_1. The same tests were performed to identify the ideal distribution of T_S/T_1 for mixed clay core and similar results were obtained (Figure 12). The histograms of Arias intensity with two types of distribution (normal and lognormal) fitted on histograms are displayed in Figure (13). These figures demonstrate that lognormal distribution has proper compatibility with the histogram of Arias intensity and the normality tests have confirmed these results. Thus, lognormal distribution was selected for the independent parameter of Arias intensity. To compare the statistical results, the distribution parameters of both normal and lognormal distributions of the input data are presented in Table (10).

Table 9. Additional accelerograms for reliability analysis.

Earthquake	T_S (sec)	Arias Intensity (m/s)	
		DBL	MCL
CAPE	0.26	0.167	0.528
KU034	0.72	4.467	14.281
NSK	0.54	1.096	3.465
STY	0.14	3.305	10.445
TAW	0.92	3.21	10.16
TTN016	0.94	4.877	15.415
DUZCE	0.22	1.934	6.114
HILLOSTER	0.1	0.802	2.541
AVAJ	0.2	0.644	2.034
FIROOZABAD	0.14	0.632	1.996
TABAS	0.32	1.83	5.773
ZAJRAN	0.16	0.393	1.243
ARCELIC	0.16	0.465	1.471
GEBZE	0.4	1.12	3.539
IZMIT	0.28	1.319	4.169
MASLAK	0.16	1.075	3.398
LUCERNE	0.08	0.997	3
SILENT	0.12	2.154	6.811
VALLEY	0.2	1.306	4.129
PALMS	0.2	0.391	1.236
GILLOERY	0.16	1.178	3.723
MONTERY	0.36	0.473	1.493
PIEDMONT	0.24	1.27	4.013
SANFRANCISCO	0.3	1.351	4.271
YERBA	0.08	0.891	2.817
MORGAN HILL	0.16	0.507	1.603
ANZA	0.08	0.558	1.763
MRREITA	0.06	0.438	1.383
LAKE HUGS	0.22	0.554	1.751
WESTMORLAND	0.32	0.244	0.771
PACOIMA	0.2	1.378	4.356
PANCHO	0.56	1.137	3.635
RIGHT WOOD	0.2	0.419	1.325
WILSON	0.16	0.393	1.242
PARK FIELD	0.16	0.631	2.017
CADAR SPRING	0.2	0.419	1.325
ALLEN	0.32	2.724	8
ISABELLA	0.32	0.433	1.37
SANFERNADO	0.16	0.483	1.526
LAKE HUGS	0.26	0.167	0.528

6.4. Probability Density Function for Dependent Parameters (Output Data)

6.4.1. Normal Distribution

First-order second-moment (FOSM) method estimates the uncertainty of the permanent displacement of an embankment against instability as a function of the variances of the stochastic input variables, such as Arias intensity and T_S/T_1. It uses Taylor's series expansion to estimate the local uncertainty of the permanent displacement at a selected expansion point. Consider that the permanent displacement (D) can be expressed as a function of stochastic input parameters Xs as:

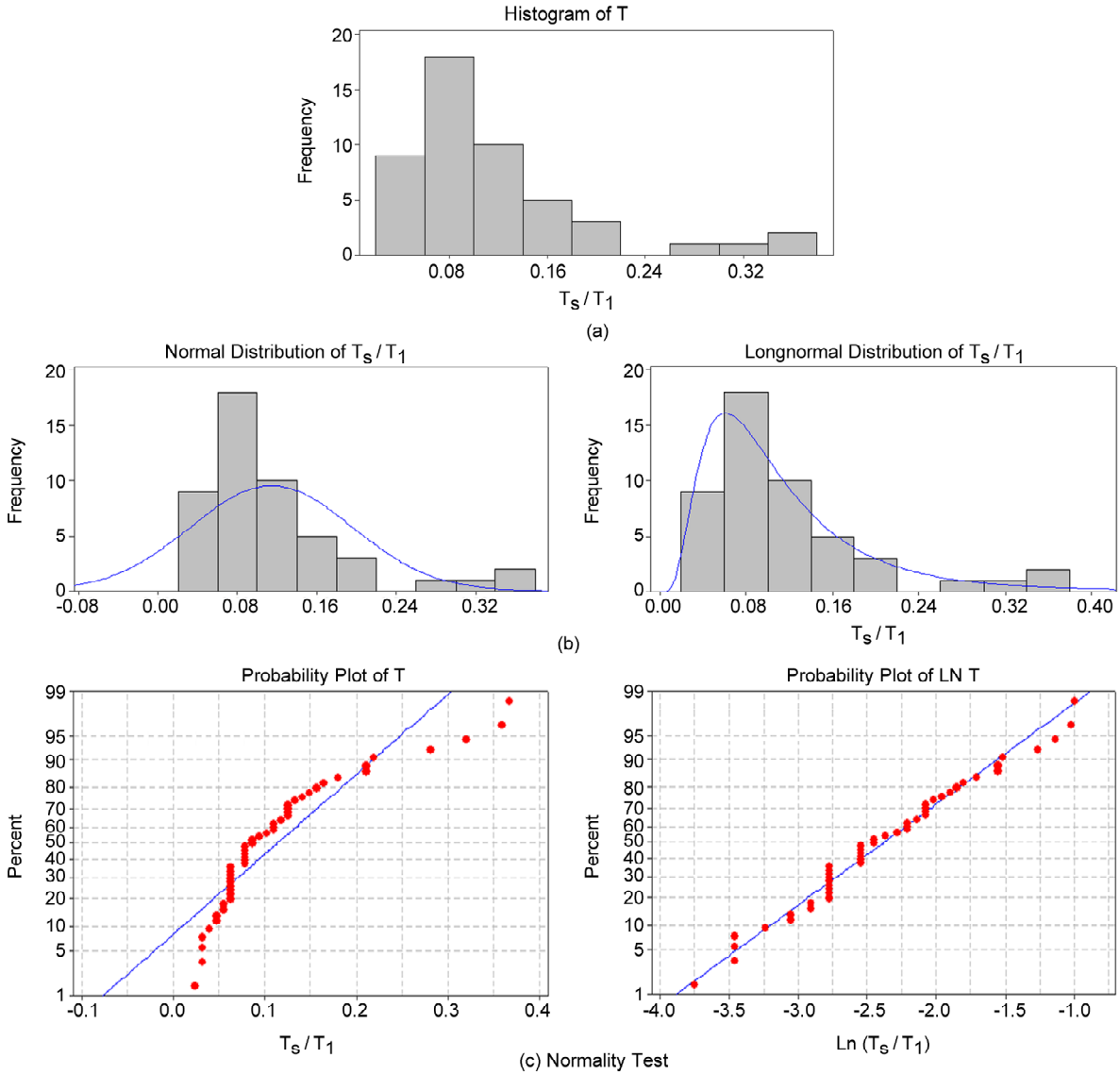

Figure 11. (a) Histogram of TS/T1 for pure clay, (b) Normal and Lognormal distribution fitted on histogram, and (c) Normality test.

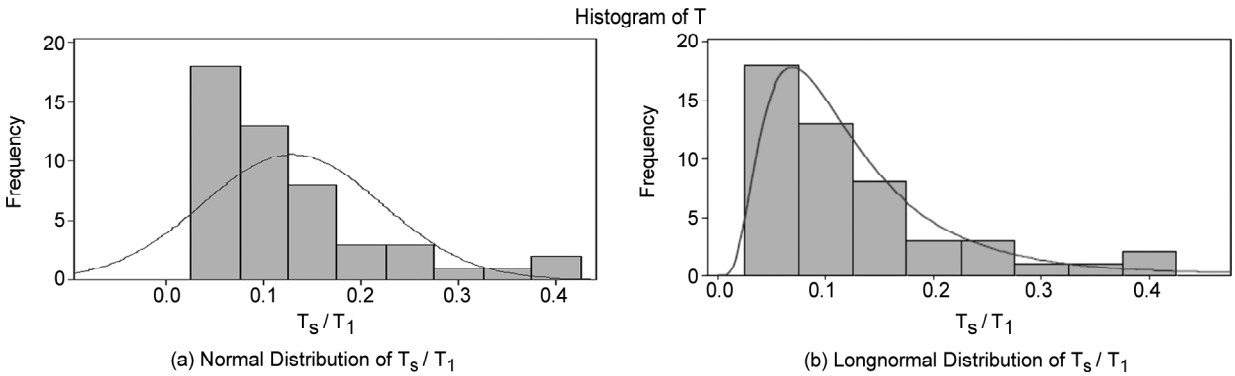

Figure 12. Histogram, Normal and Lognormal distribution fitted on histogram of mixed clay.

Table 10. (a) Lognormal distribution parameters (b) Normal distribution parameter for input data.

(a) Lognormal Distribution Parameters			(b) Normal Distribution Parameters	
Independent input parameter	**Location**	**Scale**	**Mean**	**St. Dev.**
T_S / T_1 (Pure Clay)	-2.379	0.644	0.1142	0.08167
T_S / T_1 (Mix Clay)	-2.259	0.644	0.1287	0.0921
Arias intensity (DBL)	-0.02901	0.7648	1.297	1.069
Arias intensity (MCL)	1.12	0.7627	4.079	3.373

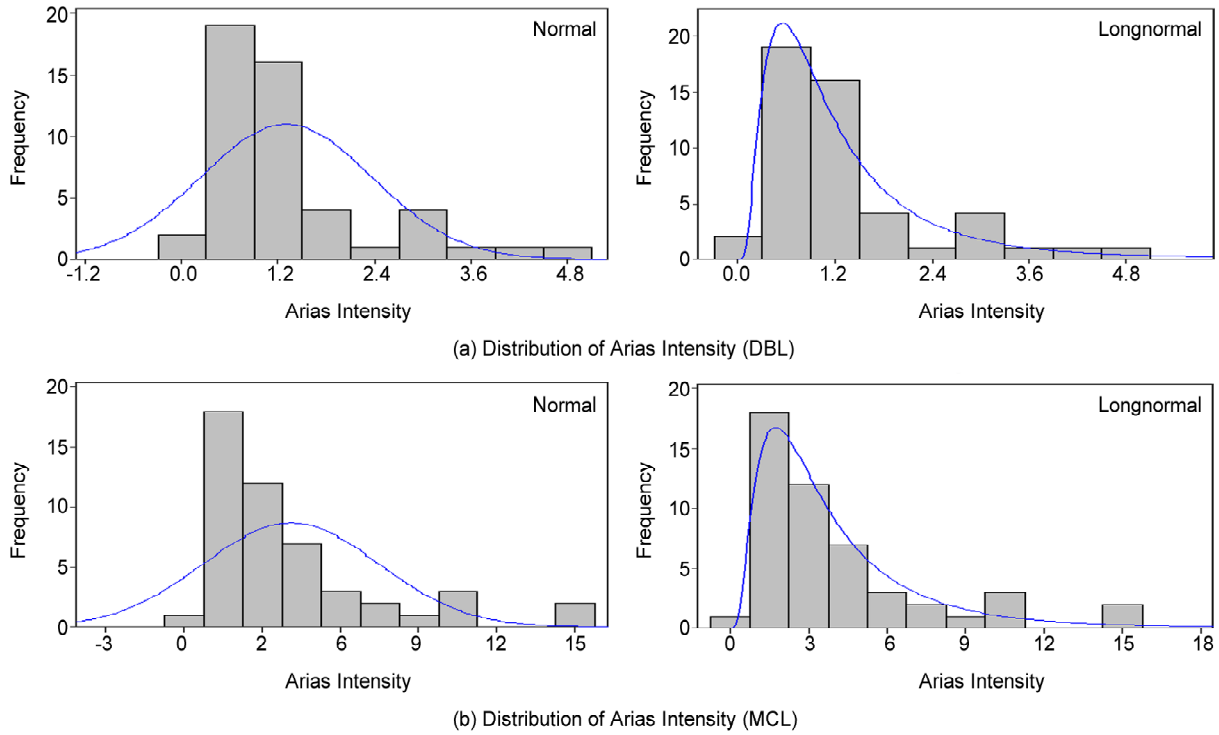

Figure 13. Histogram of Arias intensity, normal and lognormal distribution fitted on the histogram.

$$D = g\left(X^T\right) = g\left(x_1, x_2, \ldots, x_n\right) \tag{6}$$

where X is a n-dimensional vector of stochastic input parameters; the superscript (T) is the matrix or vector transpose, and g represents a functional relationship for the safety factor. In the context of the present study, $g(X^T)$ is the permanent displacement formulation using the four mentioned formulas (Table 8) of slope stability analysis via Newmark permanent displacement. The stochastic input vector X consists of the soil variables and loading variables. The FOSM method considers the first-order Taylor series expansion term of Equation (6) and the mean and variance of permanent displacement (D) can be estimated as:

$$E[D] = \mu_F \approx g\left(E[X_1], E[X_2], \ldots, E[X_n]\right) + \sum_{i=1}^{k}\sum_{j=1}^{k} \frac{\partial^2 D}{\partial X_i \partial X_j} Cov(X_i, X_j) + e \quad \text{for } i < j \tag{7}$$

$$ar[D] = \partial_D^2 \approx \sum_{i=1}^{k}\left[\left(\frac{\partial D}{\partial X_h}\right)^2 Var[X_i]\right] + 2\sum_{i=1}^{k}\sum_{j=1}^{k}\left[\left(\frac{\partial D}{\partial X_i}\frac{\partial D}{\partial X_j}\right) Cov\left[X_i X_j\right]\right] + V[e] \quad \text{for } i < j \tag{8}$$

In these equations, if input parameters have no correlations ($Cov[X_i X_j] = 0$) the parameters are uncorrelated and the equation can be written as the following equations:

$$[D] = \mu_F \approx g\left(E[X_1], E[X_2], \ldots, E[X_n]\right) + e \quad \text{for} \quad i < j \tag{9}$$

$$Var[D] = \partial_D^2 \approx \sum_{i=1}^{k}\left[\left(\frac{\partial D}{\partial X_h}\right)^2 Var[X_i]\right] + V[e] \quad \text{for} \quad i < j \tag{10}$$

where e is the error of modeling and $\frac{\partial D}{\partial X_k}$ is Fraction Derivative of each input variable. $\frac{\partial D}{\partial X_k}$ can be estimated as:

$$\frac{\partial D}{\partial X_1} = \frac{g(X_1 + \sigma_1, X_2, \ldots, X_n) - g(X_1 - \sigma_1, X_2, \ldots, X_n)}{2\sigma_1} = \frac{\Delta D_1}{2\sigma_1}, \quad \frac{\partial D}{\partial X_2} = \frac{g(X_1, X_2 + \sigma_1, \ldots, X_n) - g(X_1, X_2 - \sigma_1, \ldots, X_n)}{2\sigma_2} = \frac{\Delta D_2}{2\sigma_2}, \ldots \tag{11}$$

$$\left(\frac{\partial D}{\partial X_1}\right)^2 VarX[X_1]=\left[\frac{\Delta D}{2\sigma_1}\right]^2\sigma_1^2=\frac{1}{4}[\Delta D]^2 \quad (12)$$

Usually, two approaches are used to estimate the variance of the output parameter as approximated by the first-order second-moment method. The FOSM approach is a direct evaluation of the differential equation given in Equation (11). This is a closed form solution for *Var* (*X*). However, for most methods of slope stability analysis, such evaluation is practically impossible and inconvenient. The second approach involves a numerical approximation of the partial derivatives. This is usually used and recommended for computing the variance (uncertainty) of the seismic deformation.

Note that the four formulas (Table 8) do not have a linear relationship; therefore, a suitable approach is needed to estimate the values of statistical parameters when input parameters have a normal distribution. Herein, for this situation, FOSM method is applied to calculate the mean value and variance of permanent displacement as an output parameter. The method of calculating of statistical parameters of *D* is presented by:

$$D=90.67\times ARIAS\times\frac{T_S}{T_1}-10.79 \quad (13)$$

$$g\left(ARIAS,\frac{T_S}{T_1}\right)=90.67\times ARIAS\times\frac{T_S}{T_1}-10.79 \quad (14)$$

$$(D)\approx g\left(E(ARIAS),E\left(\frac{T_S}{T_1}\right)\right) \quad (15)$$

$$Var[D]=\sigma_D^2\approx\frac{1}{4}\sum_{i=1}^{k}[\Delta D_i]^2 \quad (16)$$

$$Var[D]=\sigma_D^2\approx\frac{1}{4}\sum_{i=1}^{k}[\Delta D_i]^2+V[e] \quad (17)$$

In this method, if n variables exist, so $2n+1$ calculation is required to estimate the mean and variance of *D*, one calculation to estimate the mean and $2n$ calculations to estimate the variance of *D*. With statistical parameters of input variables presented in Table (10b), and Equations (15) to (17), the statistical parameters of output data were estimated and presented in Table (11). As an example, the result of pure clay in DBL level is given by:

$$ARIAS\sim N(1.297,1.1449),$$
$$\frac{T_S}{T_1}\sim N(0.1142,0.0066),\ D\sim N(2.6,210.3) \quad (18)$$

Using these statistical parameters, the normal distribution of permanent displacement was determined (Figure 14).

6.4.2. Lognormal Distribution

Since the best distribution describing the input data of the current study was lognormal distribution, the suitable distribution for the output data also might be lognormal distribution. This prediction is examined herein. If the lognormal is a proper distribution of the data, then logarithm of the data has the normal distribution. Considering this fact, statistical parameters of output data were obtained. For example, in case of pure clay core at DBL the formula derived for permanent displacement obtained as follows (Table 8):

$$D=90.67\times ARIAS\times\frac{T_S}{T_1}-10.79 \quad (19)$$

$$D+10.79=90.67\times ARIAS\times\frac{T_S}{T_1} \quad (20)$$

$$Ln(D+10.79)=$$
$$Ln(90.67)+Ln(ARIAS)+Ln(\frac{T_S}{T_1}) \quad (21)$$

Table 11. Normal distribution parameters of dependent (output) data.

Material	Level of Seismic Hazard	Function (*D*)	Mean	St. Dev.
Pure Clay	DBL	$D=90.67\times ARIAS\times\frac{T_S}{T_1}-10.79$	2.64	14.63
	MCL	$D=145.1\times ARIAS\times\frac{T_S}{T_1}-35.01$	32.5	73.86
Mix Clay	DBL	$D=118.4\times ARIAS\times\frac{T_S}{T_1}-13.02$	6.75	21.5
	MCL	$D=137.8\times ARIAS\times\frac{T_S}{T_1}-12.14$	60.2	79.16

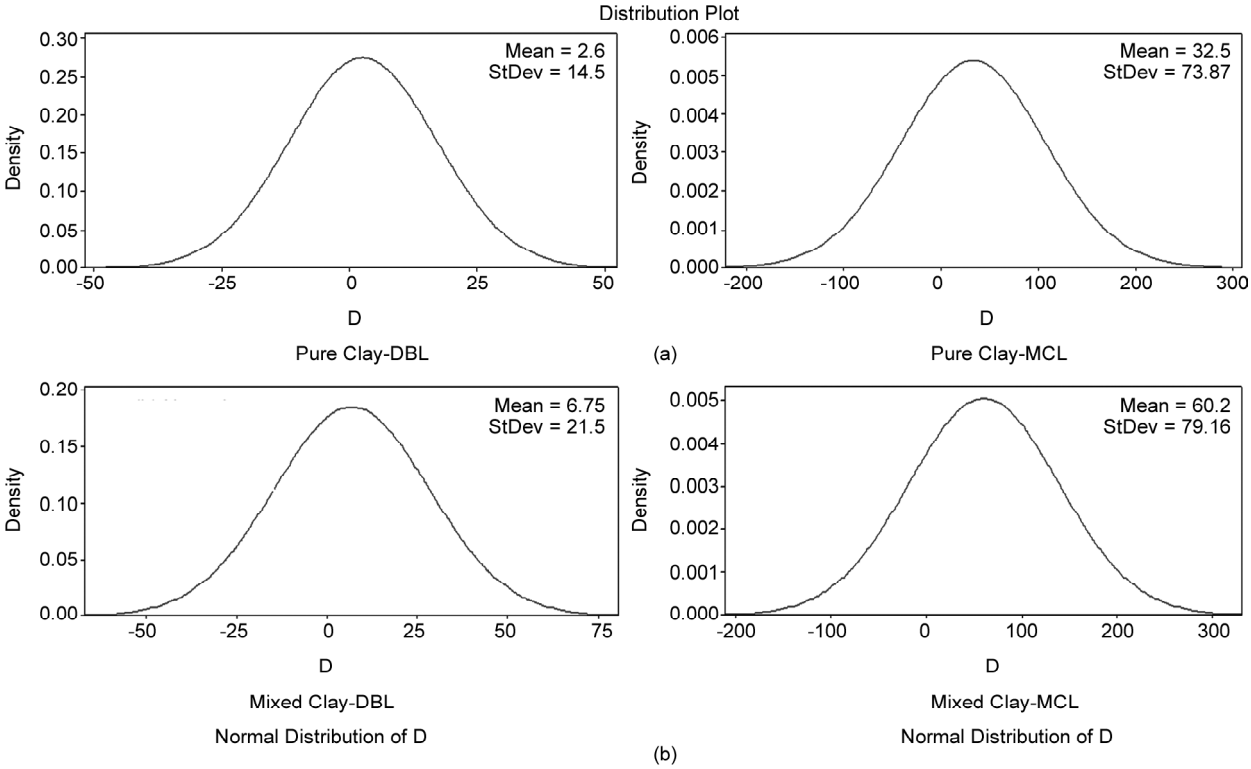

Figure 14. The Normal distribution of D for (a) pure clay, and (b) mixed clay.

While $Ln(ARIAS)$ and $Ln(\frac{T_S}{T_1})$ have the normal distribution, $Ln(D+10.79)$ has the normal distribution, so $D+10.79$ has the lognormal distribution. In this way, the statistical parameters of $Ln(D+10.79)$ are as follows:

$$Ln(ARIAS) \sim N(-0.02901, 0584) \quad (22)$$

$$Ln\left(\frac{T_S}{T_1}\right) \sim N(-2.37902, 0.415) \quad (23)$$

$$Ln(D+10.79) \sim N(2.1, 0.999) \quad (24)$$

If D^* substitutes $D+10.79$, then $Ln(D^*) \sim N(2.1, 0.999)$. The same calculation was conducted for other core materials and hazard levels and the results are shown in Table (12). Also, the graphs of lognormal distributions are presented in Figure (15).

Table 12. Lognormal distribution parameters of dependent (output) data.

Material	Level of Seismic Hazard	Function (D^*)	Location	Scale
Pure Clay	DBL	$Ln(D+10.79)$	2.1	0.999
	MCL	$Ln(D+35.01)$	3.72	0.997
Mix Clay	DBL	$Ln(D+13.02)$	2.48	0.999
	MCL	$Ln(D+12.14)$	3.787	0.996

6.5. Uncertainties and Reliability Index Calculation

The reliability index (β) is often used to express the degree of uncertainty in the calculated parameter. Reliability in seismic stability analysis is affected by various factors such as uncertainty associated with soil properties, the methods (or models) used, and the seismic loading. Herein, reliability index is calculated on the basis of permanent displacements obtained from Newmark approach, for two types of distributions, and two types of core materials at two levels of seismic hazard. Hence, a critical displacement should be defined beyond a value which causes insignificant destruction that can be repaired. Therefore, the critical displacements selected for MCL and DBL are 100 cm and 30 cm respectively [40]. Then, the value of reliability index is affected by critical displacement as:

$$\beta = \frac{D_{CRITICAL} - \mu_D}{\sigma_D} \quad (25)$$

where $D_{CRITICAL}$ is critical displacement, μ_D and σ_D are the mean and standard deviation of permanent displacement. The reliability index was determined for two types of distributions (Table 13). The reliability index is reasonably different between the two

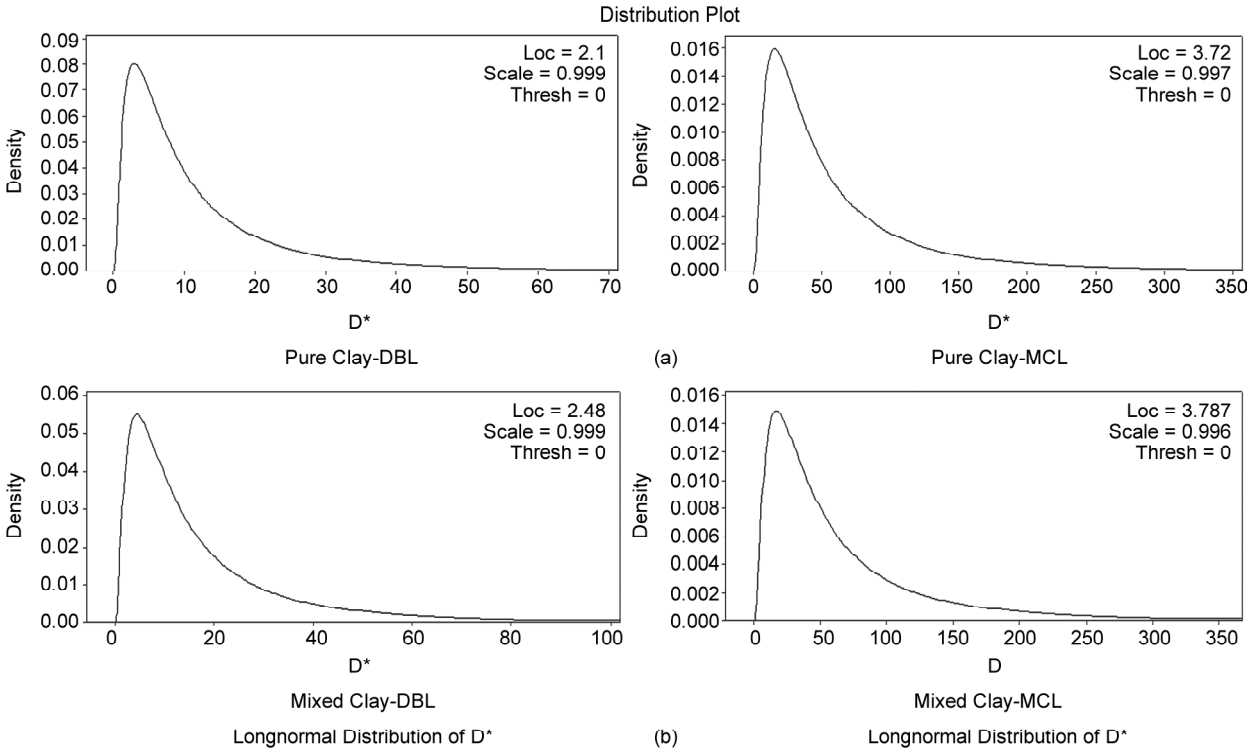

Figure 15. The Lognormal distribution of D* for (a) pure clay, and (b) mixed clay.

Table 13. Reliability index and Failure probability for (a) Lognormal distribution and (b) Normal distribution of data.

		(a) Lognormal Distribution		(b) Normal Distribution	
Material	**Level of Seismic Hazard**	**Reliability Index (β)**	**Failure Probability (P_f)**	**Reliability Index (β)**	**Probability of Failure (P_f)**
Pure Clay	DBL	1.61	5	1.87	3
	MCL	1.18	11	0.91	18
Mix Clay	DBL	1.28	9	1.08	14
	MCL	0.936	17.6	0.5	30

types of materials, and the reliability of mixed clay core is less than pure clay core. Besides, the results indicate that the normal distribution gives a lower reliability index in comparison to the lognormal distribution. In other words, the normal distribution showed an overestimation of rupture possibility in the structure. By the way, it is worth mentioning that due to some errors in the estimation of the statistical parameters of output data by the normal distribution (Figure 11c), the reliability index calculated by the lognormal distribution is more reasonable than that of the normal distribution.

6.6. Determination of Probability of Failure

Once reliability index is calculated, the probability of failure can be estimated to assess the performance of dam under earthquake loading. Equation (26) is used to estimate the probability of failure (P_f) for the lognormal distribution:

$$D + 10.79 = 90.67 \times ARIAS \times \frac{T_S}{T_1} \tag{26}$$

$$P(D > 30cm) = P(D + 10.79 > 30 + 10.79) = P(D^* > 40.79) \tag{27}$$

The results for two types of materials in MCL and DBL are presented in Figure (16). It is shown that since the probability of failure for Gotvand dam is low, this important infrastructure can have suitable performance during future earthquakes. The probability of failure is higher for mixed clay core due to the larger permanent displacement in this material. Furthermore, the probability of failure in MCL is slightly higher than in DBL.

The probability of failure was also estimated for the normal distribution, as shown in Figure (17). The P_f value for both types of distribution is summarized in Table (13). The probability of failure for the normal distribution is moderately higher

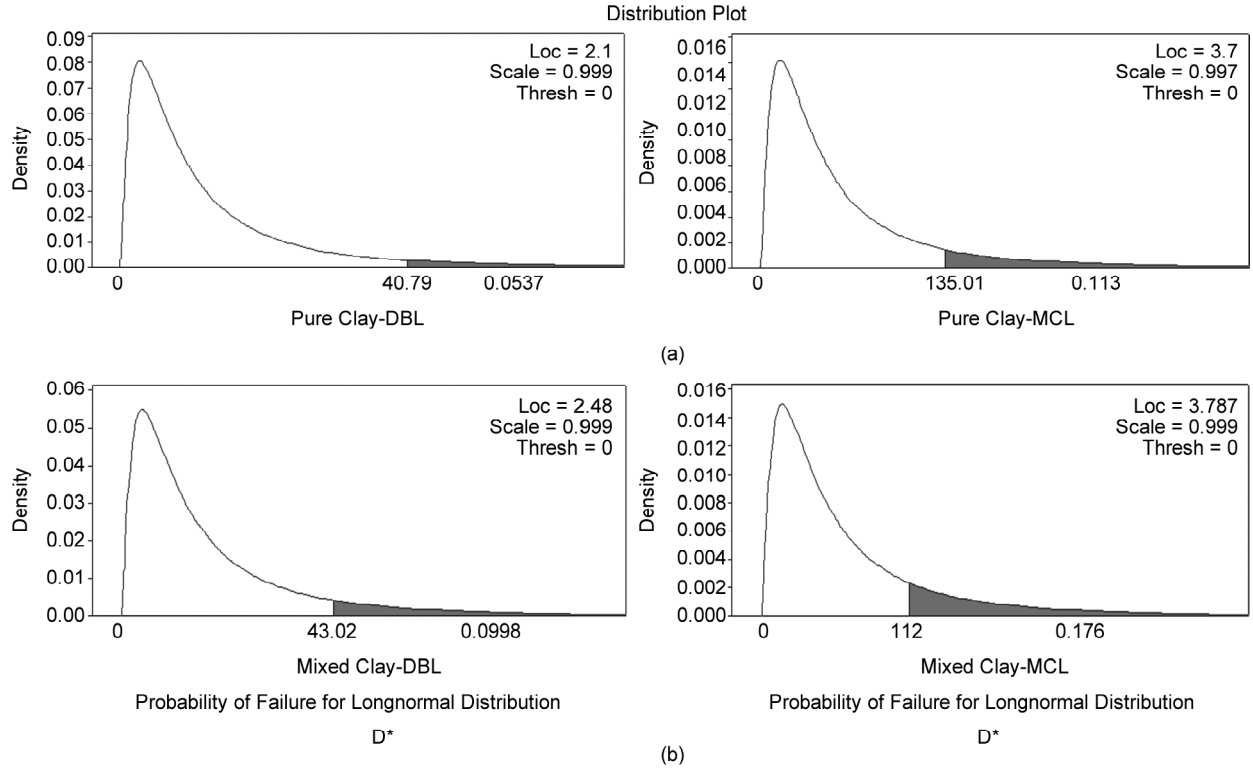

Figure 16. The Probability of Failure for Lognormal distribution for (a) pure clay, and (b) mixed clay.

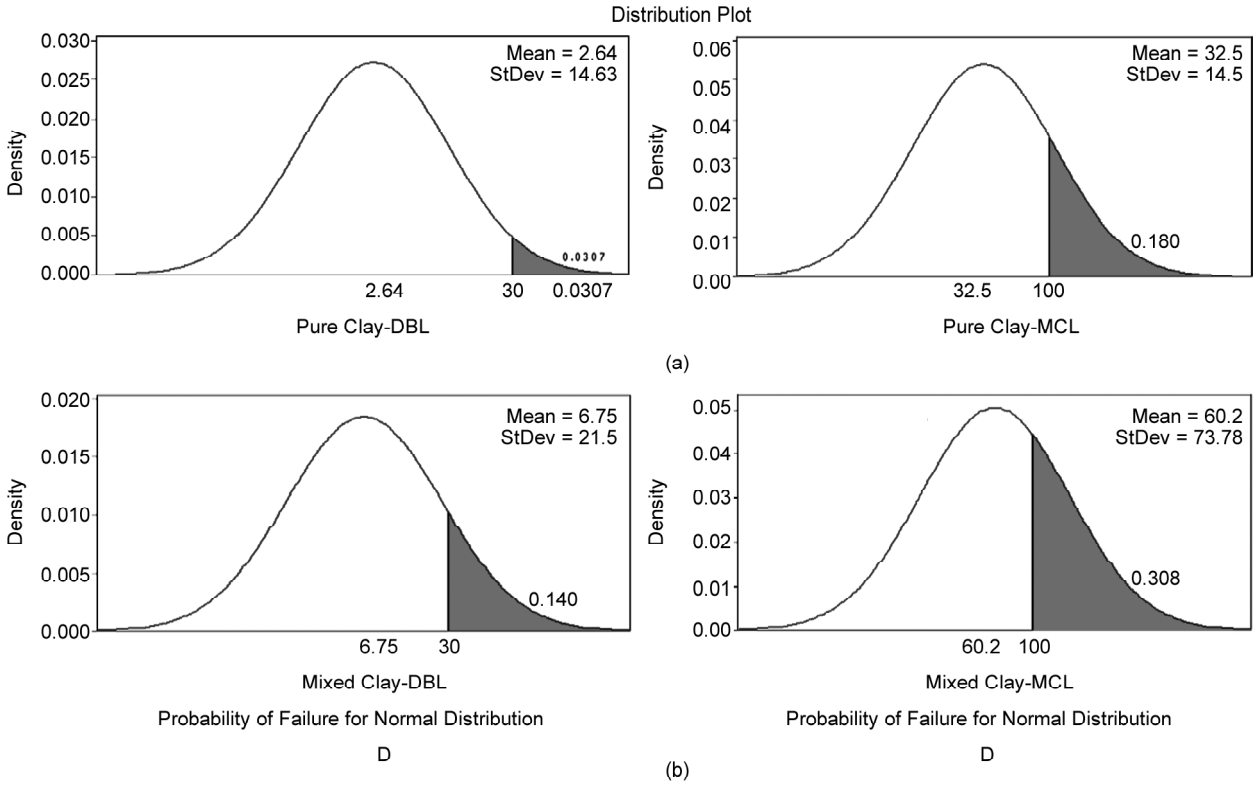

Figure 17. The Probability of Failure for Normal distribution for (a) pure clay, and (b) mixed clay.

than that for the lognormal which confirms the results obtained from the reliability index estimation.

7. Conclusion

In this study, probability theories were utilized to perform a reliability analysis in order to evaluate the seismic stability of Gotvand dam, an embankment dam constructed in the southwest of Iran. Considering different sources of uncertainties (loading and friction angle of core material) inherent in the

problem, the failure probability of dam under seismic loading was investigated. Furthermore, in order to estimate the effect of pore pressure build-up during seismic loading, two types of core materials (pure clay and mixed clay) were modeled in this research. The following conclusions were derived from the current study:

- The results of the dynamic analyses indicate that high shear strains and, consequently, high pore pressures can develop within the core when a mixed clay is used as the core material.
- The permanent displacement of the mixed clay core is moderately higher than that of the pure clay core due to the higher excess pore water pressure developed in the mixed clay core.
- The effect of friction angle variation of core material on seismic stability of Gotvand dam is not remarkable because the critical slip surface passes through the core zone in a short length.
- According to the results of reliability analysis, lognormal distribution fits best to the histogram of input and output parameters and normal distribution presents conservative results.
- Based on the presented reliability indexes and failure probabilities, using pure clay core for Gotvand dam results in higher reliability and less failure probability.
- The reliability analyses conducted based on the Newmark stability approach indicate that based on ICOLD recommendations, Gotvand dam with any of the two types of core materials is completely safe in the DBL hazard level and its performance is acceptable during MCL hazard level.

References

1. Ayyub, B.M. (1998) *Uncertainty Modeling and Analysis in Civil Engineering*. CRC Press, Boca Raton.
2. Phoon, K.-K., and Ching, J. (2017) *Risk and Reliability in Geotechnical Engineering*. CRC Press.
3. Beer, M., Zhang, Y., Quek, S.T., and Phoon, K.-K. (2013) Reliability analysis with scarce information: Comparing alternative approaches in a geotechnical engineering context. *Struct. Saf.*, **41**, 1-10.
4. Bea, R. (2006) Reliability and human factors in geotechnical engineering. *J. Geotech. Geoenvironmental Eng.*, **132**, 631-643.
5. Ranganathan, R. (1990) *Reliability Analysis and Design of Structures*. Tata McGraw-Hill.
6. Wolff, T.F. (1985) *Analysis and Design of Embankment Dam Slopes: a Probabilistic Approach*. Ph.D. Thesis, Purdue University.
7. Tang, W.H., Yucemen, M.S., and Ang, A.H.-S. (1976) Probability-based short term design of soil slopes. *Can. Geotech. J.*, **13**, 201-215.
8. Tobutt, D.C. (1982) Monte Carlo Simulation methods for slope stability. *Comput. Geosci.*, **8**, 199-208.
9. Wang, Y., Cao, Z., and Au, S.-K. (2011) Practical reliability analysis of slope stability by advanced Monte Carlo simulations in a spreadsheet. *Can. Geotech. J.*, **48**, 162-172.
10. Chowdhury, R.N. and Xu, D.W. (1994) Slope system reliability with general slip surfaces. *Soils Found*, **34**, 99-105.
11. Christian, J.T., Ladd, C.C., and Baecher, G.B. (1994) Reliability applied to slope stability analysis. *J. Geotech. Eng.*, **120**, 2180-2207.
12. Al-Homoud, A.S. and Tahtamoni, W.W. (2000) Reliability analysis of three-dimensional dynamic slope stability and earthquake-induced permanent displacement. *Soil Dyn. Earthq. Eng.*, **19**, 91-114.
13. Juang, C.H., Lee, D.H., and Sheu, C. (1992) Mapping slope failure potential using fuzzy sets. *J. Geotech. Eng.*, **118**, 475-494.
14. Habibagahi, G. and Shahgholian, R. (2002) Reliability analysis of rock slopes using theory of fuzzy sets. *Proc. of the 8th International Symposium on Numerical Models in Geomechanics*, Rome, Italy, 547-551.
15. Holtz, W.G. (1961). Triaxial shear characteristics of clayey gravel soils. *Proc. of the Fifth International Congress on Soil Mechanics and Foundation Engineering*, Paris, France, 143-149.
16. Irfan, T.Y., and Tang, K.Y. (1992) Effect of the

coarse fractions on the shear strength of colluvium. *Geo Report 23*, Geotechnical Engineering Office, Civil Engineering Dept., Hong Kong.

17. Schultze, E. (1957) Large-scale shear tests. *Proc. of the Fourth International Conference on Soil Mechanics and Foundation Engineering*, London, UK, 193-199.

18. Jafari, M.K. and Shafiee, A. (2004) Mechanical behavior of compacted composite clays. *Can. Geotech. J.*, **41**, 1152-1167.

19. Seco e Pinto, P.S. (1993) Dynamic analysis of embankment dams. *Proc. of the Seminar on Soil Dynamics and Geotechnical Earthquake Engineering*, Lisbon, Portugal, A.A. Balkema, 159-269.

20. Shafiee, A. (2008) Effect of core composition on seismic stability of earth dams. *Proc. Inst. Civ. Eng. Geotech. Eng.*, **161**, 283-290.

21. Shafiee, A., Bahador, M., and Bahrami, R. (2008) Application of fuzzy Set theory to evaluate the effect of pore pressure build-up on the seismic stability of Karkheh Dam. *Iran. J. Earthq. Eng.*, **12**, 1296-1313.

22. Cotecchia, V. (1987) *Earthquake-Prone Environments, in Slope Stability, Geotechnical Engineering and Geomorphology*. John Wiley & Sons, Inc., New York, USA, 278-330.

23. Kramer, S.L. (1996) G*eotechnical Earthquake Engineering*. Pearson, Upper Saddle River, N.J.

24. Newmark, N.M. (1965) Effects of earthquakes on dams and embankments. *Géotechnique*, **15**, 139-160.

25. MGCE (1998) *Technical Report on Foundation and the Body of Kharkheh Dam*. Mahab Ghods Consulting Engineering Co. (MGCE), Tehran, Iran.

26. MGCE (2005) *Seismicity, Seismotechtonics and Seismic Hazard Analysis, Upper Gotvand Hydroelectric Dam Project*. Iran Water & Power Resources Development Co. (IWPC), Tehran, Iran.

27. Makdisi, F.I. and Seed, H.B. (1977) *A Simplified Procedure for Estimating Earthquake-induced Deformations in Dams and Embankments*. College of Engineering, University of California, Earthquake Engineering Research Center.

28. Jibson, R.W. (1993) Predicting earthquake-induced landslide displacements using Newmark's sliding block analysis. *Transp. Res. Rec.*, 9-17.

29. Wilson, R.C. and Keefer, D.K. (1985) 'Predicting areal limits of earthquake-induced landsliding'. In: *Evaluating Earthquake Hazards in the Los Angeles Region*; An Earth-Science Perspective, J.I. Ziony (ed).

30. Jones, A.L., Kramer, S.L., and Arduino, P. (2002) *Estimation of Uncertainty in Geotechnical Properties for Performance-Based Earthquake Engineering*. Pacific Earthquake Engineering Research Center, Berkeley, USA.

31. Mrabet, Z. (1999) Reliability Analysis of homogeneous earth fills-A new approach. *Proc. of the 8th International Conference on Applications of Statistics and Probability in Civil Engineering*, Sydney, Australia, Balkema, 499-507.

32. Mrabet, Z. and Bouayed, A. (2000) Reducing uncertainty on the results of reliability analysis of earth fills using stochastic estimations. *Proc. of the Second International Conference on Computer Simulation in Risk Analysis and Hazard Mitigation*, Bologna, Italy, 203-214.

33. Mrabet, Z. (2004) Some aspect on reliability in geotechnical engineering. *Proc. of the 4th International Conference on Computer Simulation in Risk Analysis and Hazard Mitigation*, Greece, 75-84.

34. Spanos, P.D. and Ghanem, R. (1989) Stochastic Finite element expansion for random media. *J. Eng. Mech.*, **115**, 1035-1053.

35. Fenton, G.A. (1990) *Simulation and Analysis of Random Fields*. Princeton University Princeton, NJ.

36. Smith, I.M. and Griffiths, D.V. (1998) *Programming the Finite Element Method*. John Willey & Sons Ltd., West Sussex, UK.

37. Mrabet, Z. (2002) Reliability analysis of earth fills using stochastic estimation methods. *Proc. of 3rd International Conference on Mathematical Methods in Reliability*, Trondheim, Norway, 17-20.

38. Mrabet, Z. and Bouayed, A. (2003) Probabilistic risk assessment of homogeneous earth dams. *Proc. of the 9th International Conference on Applications of Statistics and Probability in Civil Engineering*, San Francisco, California, 367-372.

39. Benjamin, J.R. and Cornell, C.A. (1970) *Probability, Statistics, and Decision for Civil Engineers*. McGraw-Hill, New York.

40. ICOLD (1989) *Selecting Seismic Parameters for Large Dams, Guidelines, Bulletin 72*.